Glucose Deprivation Regulates K_{ATP} Channel Trafficking via AMP-Activated Protein Kinase in Pancreatic β-Cells

Ajin Lim,[1,2] Sun-Hyun Park,[1,2] Jong-Woo Sohn,[1,2] Ju-Hong Jeon,[2] Jae-Hyung Park,[3] Dae-Kyu Song,[3] Suk-Ho Lee,[1,2] and Won-Kyung Ho[1,2]

OBJECTIVE—AMP-activated protein kinase (AMPK) and the ATP-sensitive K^+ (K_{ATP}) channel are metabolic sensors that become activated during metabolic stress. AMPK is an important regulator of metabolism, whereas the K_{ATP} channel is a regulator of cellular excitability. Cross talk between these systems is poorly understood.

RESEARCH DESIGN AND METHODS—Rat pancreatic β-cells or INS-1 cells were pretreated for 2 h at various concentrations of glucose. Maximum K_{ATP} conductance (G_{max}) was monitored by whole-cell measurements after intracellular ATP washout using ATP-free internal solutions. K_{ATP} channel activity (*NPo*) was monitored by inside-out patch recordings in the presence of diazoxide. Distributions of K_{ATP} channel proteins (Kir6.2 and SUR1) were examined using immunofluorescence imaging and surface biotinylation studies. Insulin secretion from rat pancreatic islets was measured using an enzyme immunoassay.

RESULTS—G_{max} and *NPo* in cells pretreated with glucose-free or 3 mmol/l glucose solutions were significantly higher than in cells pretreated in 11.1 mmol/l glucose solutions. Immunofluorescence imaging and biotinylation studies revealed that glucose deprivation induced an increase in the surface level of Kir6.2 without affecting the total cellular amount. Increases in G_{max} and the surface level of Kir6.2 were inhibited by compound C, an AMPK inhibitor, and siAMPK transfection. The effects of glucose deprivation on K_{ATP} channels were mimicked by an AMPK activator. Glucose deprivation reduced insulin secretion, but this response was attenuated by compound C.

CONCLUSIONS—K_{ATP} channel trafficking is regulated by energy status via AMPK, and this mechanism may play a key role in inhibiting insulin secretion under low energy status. ***Diabetes*** **58:2813–2819, 2009**

ATP-sensitive K^+ (K_{ATP}) channels are metabolic sensors that couple cellular energy status to electrical activity and play key roles in energy-dependent insulin secretion in pancreatic β-cells (1). The molecular mechanisms underlying the regulation of K_{ATP} channel activity have been investigated extensively. Adenine nucleotides are well known to induce K_{ATP} channel closure by binding to the pore-forming subunit Kir6.2 (2), yet activate channel opening by interacting with the regulatory subunit SUR in a Mg^{2+}-dependent manner (3,4). Therefore, energy-dependent regulations of K_{ATP} currents are believed to be because of the direct effects of these nucleotides on K_{ATP} channel gating. However, the total conductance of an ion channel is determined not only by open probabilities but also by the available channel numbers. Our work addresses the latter, focusing on whether K_{ATP} channel numbers at the surface membrane can be regulated by cellular energy status.

The importance of the trafficking mechanism for K_{ATP} channels was first recognized in studies on mutant channels involved in insulin secretion disorders. For some mutations causing congenital hyperinsulinism the forward trafficking is impaired (5,6), whereas mutations that affect the signaling motif responsible for endocytic trafficking cause neonatal diabetes (7). The trafficking of normal K_{ATP} channels has been reported to be regulated in several recent studies. High-glucose conditions have led to the recruitment of K_{ATP} channels to the β-cell plasma membrane in a Ca^{2+} and PKA-dependent manner, resulting in an increase in K_{ATP} currents (8), whereas a protein kinase C activator facilitated endocytic trafficking of K_{ATP}, resulting in decreased K_{ATP} currents (9). These studies suggest that regulation of the surface density of K_{ATP} channels is a dynamic process involving various steps of trafficking and that each step is subject to regulation by various cellular signaling mechanisms. However, the involvement of energy-dependent signaling mechanisms in the regulation of K_{ATP} channel trafficking has not been fully studied.

AMP-activated protein kinase (AMPK) is an evolutionarily conserved metabolic sensor that is activated under conditions of energy deficiency and plays key roles as a regulator of energy metabolism (10). Recent studies have found that AMPK also plays important roles in coupling membrane transport to cellular metabolism (11). AMPK has been shown to upregulate glucose transporters and fatty acid translocase (12) but downregulate ion-transport proteins such as cystic fibrosis transmembrane conductance regulator (CFTR) Cl^- channels (13) and epithelial Na^+ channels (14). Although the mechanisms involved in these effects are not fully understood, AMPK-dependent downregulation of CFTR has been shown to be associated with decreased CFTR surface expression in colonic epithelium (15), whereas AMPK increases GLUT4 translocation to the sarcolemma in skeletal and cardiac muscle (16,17). These results may suggest that AMPK regulates the mechanisms involved in the trafficking of surface proteins.

Pancreatic β-cells are a key player in the regulation of whole-body energy balance. They are specialized to synthesize and secrete insulin, a key anabolic hormone of the body. Insulin secretion is controlled tightly by blood

From the [1]National Research Laboratory for Cell Physiology, Seoul National University College of Medicine, Seoul, Korea; the [2]Department of Physiology, Seoul National University College of Medicine, Seoul, Korea; and the [3]Department of Physiology and Chronic Disease Research Center, Keimyung University School of Medicine, Daegu, Korea.

Corresponding author: Won-Kyung Ho, wonkyung@snu.ac.kr.

Received 23 April 2009 and accepted 12 August 2009. Published ahead of print at http://diabetes.diabetesjournals.org on 31 August 2009. DOI: 10.2337/db09-0600.

glucose concentration, and the ability of the K_{ATP} channel to couple its activity to cellular energy status is generally believed to be responsible for glucose-dependent insulin secretion. AMPK activity is also controlled by glucose concentration in insulin-secreting cells (18), but little is known about the roles of AMPK in pancreatic β-cells. In the present study, we investigated whether AMPK activation contributes to the activation of K_{ATP} channels in pancreatic β-cells and INS-1 cells. We found that the activation of AMPK by glucose deprivation induces an increase in the surface levels of K_{ATP} channels, and this increase contributes to the increased K_{ATP} conductance.

RESEARCH DESIGN AND METHODS

INS-1 cells and rat pancreatic β-cell culture. INS-1 cells (passage 5–45) were cultured in RPMI1640 medium (Sigma) containing 11.1 mmol/l D-glucose supplemented with 10% heat-inactivated FBS, 10 mmol/l HEPES, 100 units/ml penicillin, 100 mg/ml streptomycin, 1 mmol/l sodium pyruvate, and 50 μmol/l β-mercaptoethanol at 37°C in a humidified incubator containing 5% CO_2. Cells were grown in 12-well plates at a density of 5×10^4 per well for electrophysiology and on 12-mm poly-L-lysine–coated coverslips for immunocytochemistry.

Pancreatic β-cells were isolated from the islets of Langerhans of Sprague-Dawley rats weighing 200–300 g. Animals were anesthetized with pentobarbital sodium (50 mg/kg, i.p.). All procedures were approved by the Institute of Laboratory Animal Resources at Seoul National University. Islets were isolated after digesting the pancreas by injecting 1 mg/ml collagenase dissolved in Hank's balanced salt saline (HBSS, Sigma) solution into pancreatic ducts. Collected islets were dispersed mechanically into single cells in Ca^{2+}-free Krebs-Ringer bicarbonate buffer (KRBB, Sigma) and then plated onto poly-L-lysine–coated coverslips and cultured for 4–5 days in RPMI1640 medium containing 11.1 mmol/l D-glucose, 100 units/ml penicillin, and 100 mg/ml streptomycin. We confirmed by poly(ADP-ribose) polymerase cleavage assay that cell viability was not affected after glucose deprivation for 2 h.

Electrophysiology. K_{ATP} channel currents were monitored at room temperature using a standard whole-cell or inside-out patch-clamp technique with an EPC-10 amplifier and Pulse software (version 8.67; Heka Electronik) and analyzed using IGOR software. The cell-attached patch technique was used to measure unitary K_{ATP} currents with an Axopatch 200B amplifier and analyzed with pCLAMP software (Axon Instruments). Patch electrodes were pulled from borosilicate glass capillaries to obtain a resistance between 2 and 5 mol/lΩ. The internal solution for whole-cell experiments contained (in millimoles per liter) 30 KCl, 110 K-aspartate, 2.6 $CaCl_2$, 10 HEPES (pH 7.2 with KOH), 0.5 EGTA, and 5 EDTA. The free Ca^{2+} concentration was calculated to be ~24 nmol/l. The bath solution for whole-cell and cell-attached patch recordings contained (in millimoles per liter) 137 NaCl, 5.6 KCl, 10 HEPES (pH 7.4 with NaOH), 0.5 $MgCl_2$, and 1.8 $CaCl_2$. Compound C (Calbiochem) and 5-aminoimidazole-4-carboxamide ribonucleoside (AICAR, Calbiochem) were added during pretreatment as indicated in the text and included during current recordings. For inside-out and cell-attached patch recordings, pipettes were filled with a solution containing (in millimoles per liter) 140 KCl, 2.6 $CaCl_2$, 1 $MgCl_2$, and 10 HEPES (pH 7.2 with KOH); upon patch excision in inside-out experiments, bath solutions were changed to a solution containing (in millimoles per liter) 107 KCl, 1 $CaCl_2$, 2 $MgCl_2$, 10 HEPES, and 11 EGTA (pH 7.2 with KOH).

Fluorescence staining of K_{ATP} channels. Cells were fixed with 4% paraformaldehyde in PBS for 15 min. For K_{ATP} channel staining, cells were permeabilized with 0.25% Triton X-100 in PBS for 10 min, blocked with 2% donkey serum in PBS for 30 min at room temperature, and incubated with rabbit anti-Kir6.2 (1:50, Santa Cruz Biotechnology) and goat anti-SUR1 (1:50, Santa Cruz Biotechnology) and rabbit anti Kir2.1 (1:50, Santa Cruz Biotechnology) antibodies overnight at 4°C. The subcellular localizations of Kir6.2 were assessed using Alexa488-conjugated anti-rabbit IgG antibody (488-nm excitation, 1:100, Invitrogen) and Cy5-conjugated anti-goat IgG (633-nm excitation, 1:100, Jackson ImmunoResearch) antibodies, respectively. Images were acquired by confocal microscopy (Leica, Germany; FluoView 1000, Olympus) using a 63× oil-immersion objective. The same instrument settings were used for each experiment, and all experiments were repeated at least three times. Because we did not identify β-cells using insulin antibody, we could not entirely exclude the possibility that α-cells or δ-cells were included in our observation.

Surface biotinylation and Western blotting. The surface and total expression levels of Kir6.2 were determined by Western blot analysis using an antibody to Kir6.2 (1:1,000, Santa Cruz Biotechnology). The surface protein fractions of INS-1 cells were assessed using surface biotinylation EZ-Link sulfo-NHS-SS-biotin kits (Pierce). To verify consistent amounts of surface proteins, the membrane probed by Kir6.2 primary antibody was washed for 2 h and examined by immunoblot using an antibody to Kir2.1 (1:1,000, Santa Cruz Biotechnology). Total protein was prepared by incubating cells with RIPA buffer, and proteins were resolved by 12% SDS-PAGE. Further details are described in the online appendix, available at http://diabetes.diabetesjournals.org/cgi/content/full/db09-0600/DC1.

Measurement of insulin secretion from pancreatic islets. Insulin secretion from rat pancreatic islets was measured by enzyme immunoassay (ELISA kits, Mercodia). Changes in insulin secretion in response to glucose deprivation were monitored using the batch incubation method by collecting samples at 30-min intervals. Each independent batch contained 10 size-matched islets. Further details are described in the online appendix.

Statistical analysis. All data are presented as means ± SE. All statistical analyses were performed using ANOVA, and $P < 0.05$ was considered to be significant.

RESULTS

Pretreatment in low glucose solution increases K_{ATP} conductance. To investigate the roles of energy-dependent signaling mechanisms in K_{ATP} channel regulation, we pretreated INS-1 cells with different concentrations of glucose (0 mmol/l for glucose-deprived [GD], 3 mmol/l for low glucose [3G], 11.1 mmol/l for control [11G]) for 2 h at room temperature before K_{ATP} currents were recorded. The experimental protocol used is illustrated in Fig. 1*A*. To induce the maximal activation of K_{ATP} channels, we dialyzed the cells with ATP-free internal solutions and monitored changes in cell conductance in response to the washout of intracellular ATP by applying hyperpolarizing pulses to −130 mV, from a holding potential of −70 mV every 10 s (Fig. 1*B*). We confirmed that the increases in currents under these conditions were because of K_{ATP} channel activation by testing the effect of glibenclamide, a selective K_{ATP} channel blocker (data not shown). For reliable measurements of maximum current amplitude, the K_{ATP} current rundown was minimized by adding 5 mmol/l EDTA to the internal solutions (19). Upon patch break-in, several minutes passed until the whole-cell conductance increased rapidly and reached the maximum level. This delay was longer in cells pretreated with 11G than that in cells pretreated with 3G or the GD solution. This observation was expected because the initial ATP concentrations would be higher in 11G-treated cells, so that ATP washout would take longer. However, it was surprising to find that the amplitudes of K_{ATP} currents at their maximum activation were much smaller in 11G-treated cells than in 3G- or GD-treated cells (Fig. 1*B*). For statistical comparison, the maximum K_{ATP} conductance (G_{max}), calculated by measuring the difference in current amplitudes between −130 and −70 mV, was normalized to the cell capacitance (C_m). The mean value for normalized G_{max} in GD-treated cells (2.48 ± 0.24 nS/pF) was similar to that in 3G-treated cells (2.28 ± 0.12 nS/pF), whereas that in 11G-treated cells (0.33 ± 0.05 nS/pF) was significantly less than that in GD- or 3G-treated cells ($P < 0.001$). No significant difference in C_m was observed among 11G, 3G, and GD-treated cells (12.01 ± 0.28 pF; $n = 130$).

It may be argued whether the lower G_{max} in 11G-treated cells was because of insufficient washout of cellular factors that could suppress K_{ATP} channels. To exclude this possibility, we used inside-out excised patch recordings, yet significant differences in K_{ATP} channel activities were still observed between 11G- and GD-treated cells. The mean value for *NPo* obtained in the presence of diazoxide

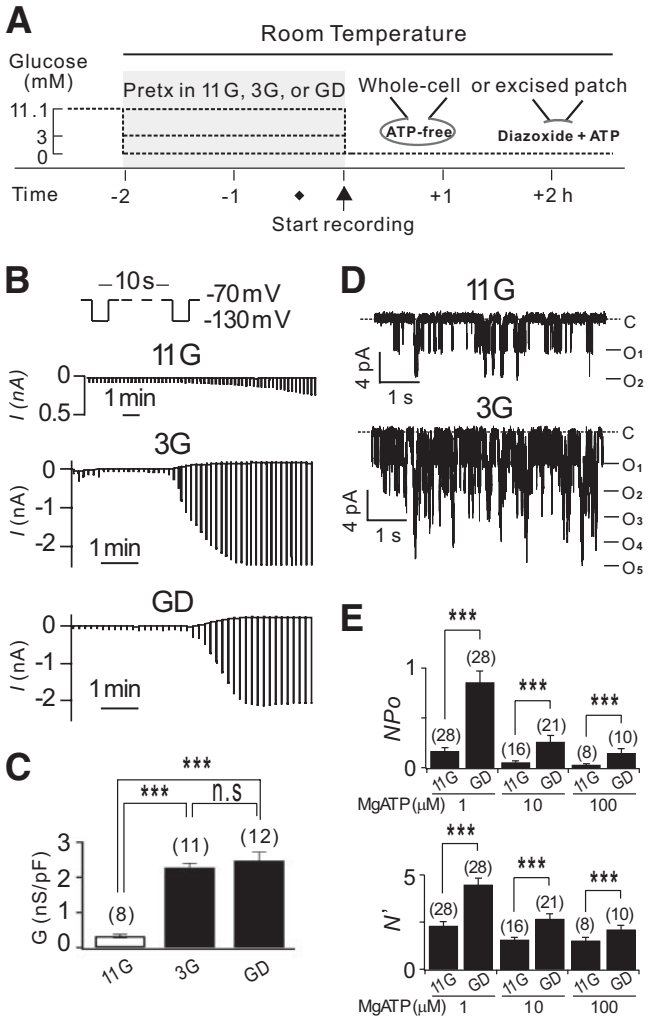

FIG. 1. Effect of glucose pretreatment concentration on K_{ATP} currents in INS-1 cells. *A*: Schematic diagram of the experimental protocols used for treating cells before current recording. 11G, 3G, and GD represent 11.1 mmol/l, 3 mmol/l, and 0 mmol/l glucose, respectively. *B*: Representative recordings of K_{ATP} whole-cell currents in 11G-, 3G-, and GD-treated INS-1 cells. Whole-cell current traces were obtained by hyperpolarizing pulses to −130 mV (500 ms) from a holding potential of −70 mV every 10 s. *C*: Mean conductance normalized to cell capacitance (nS/pF) measured at peak activation from 11G-, 3G-, and GD-treated cells (n = 8, 11, and 12, respectively). *D*: Single K_{ATP} channel currents recorded at −60 mV from an inside-out patch obtained from 11G- (*upper panel*) and GD-treated INS-1 cells (*lower panel*) exposed to 0.25 mmol/l diazoxide in the presence of 1 μmol/l MgATP. *C*, closed level. *O*, opened level. *E*: *Upper panel*: Mean K_{ATP} channel activity (*NPo*) in 11G- and GD-treated cells. Mean values for *NPo*; 0.16 ± 0.04 (n = 28) in 11G and 0.86 ± 0.12 (n = 28) in GD, 0.05 ± 0.02 (n = 16) in 11G and 0.25 ± 0.06 (n = 28) in GD, 0.04 ± 0.01 (n = 8) in 11G and 0.15 ± 0.04 (n = 10) in GD when the cells were exposed to 0.25 mmol/l diazoxide in the presence of 1 μmol/l, 10 μmol/l, and 100 μmol/l MgATP, respectively. *Lower panel*: Maximum number of channels opened at the same time (*N'*) within the excised patch pipette. Statistical significance was evaluated by an unpaired t test and one-way ANOVA. ***P < 0.001.

(0.25 mmol/l) and ATP in GD-treated cells was about five times larger than that in 11G-treated cells (Fig. 1*D*). Furthermore, the maximum number of channels opened at the same time in a patch membrane (*N'*) was significantly more in GD-treated cells compared with 11G-treated cells. The differences between 11G- and GD-treated cells were unaffected by varying ATP concentrations (Fig. 1*E*). These results support the hypothesis that some energy-dependent signaling mechanism(s) activated during the pretreatment in 3G or GD was required to activate K_{ATP} conductance to its full capacity. There was no evidence that the ATP sensitivity and gating kinetics (mean open time) of the K_{ATP} channels were affected by glucose deprivation (supplementary Figs. S1 and S2). We next investigated which signaling mechanism is responsible for the GD-induced increases in K_{ATP} channels.

AMPK activation underlies GD-induced increases in K_{ATP} conductance. The activation of AMPK by glucose deprivation has been reported in insulin-secreting cell lines (18). To confirm that AMPK was activated in INS-1 cells by glucose deprivation or low glucose (3 mmol/l), Western blot analysis was performed using a phosphorylation-specific antibody. The levels of the phosphorylated AMPKα (pThr^{172}) increased similarly for cells in 0 or 3 mmol/l glucose solutions, reaching maximum levels after 2 h at room temperature and 30 min at 37°C, whereas the total AMPK levels were unaffected (Fig. 2*A*). We tested the involvement of AMPK in GD-induced increases in K_{ATP} channel activities using compound C (an AMPK inhibitor) (20), AMPK siRNA transfection, and AICAR (an AMPK activator) (21). K_{ATP} current activation was almost completely abolished in cells pretreated with compound C (10 μmol/l) for 30 min before current recording in glucose-free solution (GD + CC; Fig. 2*B*, *upper panel*), and G_{max} (0.22 ± 0.04 nS/pF; n = 11) became similar to the background conductance measured in the presence of glibenclamide (0.12 ± 0.03 nS/pF). We confirmed that the K_{ATP} channel activity recorded by inside-out patches was not affected by compound C applied to the internal side of the membrane (supplementary Fig. S3*B*), but K_{ATP} current activation in GD-treated cells in whole-cell recordings was abolished by adding compound C to internal solutions (supplementary Fig. S3*A*). These results indicated that compound C inhibited K_{ATP} channels not directly but by inhibiting intracellular mechanisms and that this inhibitory effect appeared in a relatively short period. Furthermore, K_{ATP} current activation in 11G-treated cells increased significantly when AICAR (0.5 mmol/l) was added 20 min before current recording (Fig. 2*B*, *middle panel*), becoming indistinguishable from K_{ATP} current activation of GD-treated cells. The application of AICAR to GD-treated cells did not induce further increases in G_{max}. The effects of compound C and AICAR on K_{ATP} channel activities observed in inside-out recordings (Fig. 2*C*) were similar to their effects on whole-cell K_{ATP} conductance. The finding that the effect of glucose deprivation on K_{ATP} channels was inhibited by compound C and mimicked by AICAR indicated that AMPK was responsible for the GD-induced increases in K_{ATP} conductance. We confirmed that the effects of GD, compound C, and AICAR on K_{ATP} conductance were similarly observed in pancreatic β-cells (supplementary Fig. S4).

The involvement of AMPK in K_{ATP} channel regulation was further confirmed in INS-1 cells transfected with both α1- and α2-AMPK siRNA (siAMPK) (RESEARCH DESIGN AND METHODS are described in the online appendix). The total expression of the α-subunit of AMPK in cells transfected with siAMPK was significantly lower than that in cells transfected with an equal concentration of scrambled siRNA (Scr; supplementary Fig. S5*A*). For patch-clamp experiments, green fluorescence protein was cotransfected, and green fluorescence protein-positive cells were selected for current recordings. Transfection of Scr did not appear to affect the K_{ATP} current in GD-treated cells (Fig. 2*D*, *lower panel*), and the normalized G_{max} was similar to that in untransfected cells (Fig. 1). In contrast, the K_{ATP} current activation in cells transfected with siAMPK was negligible in seven of

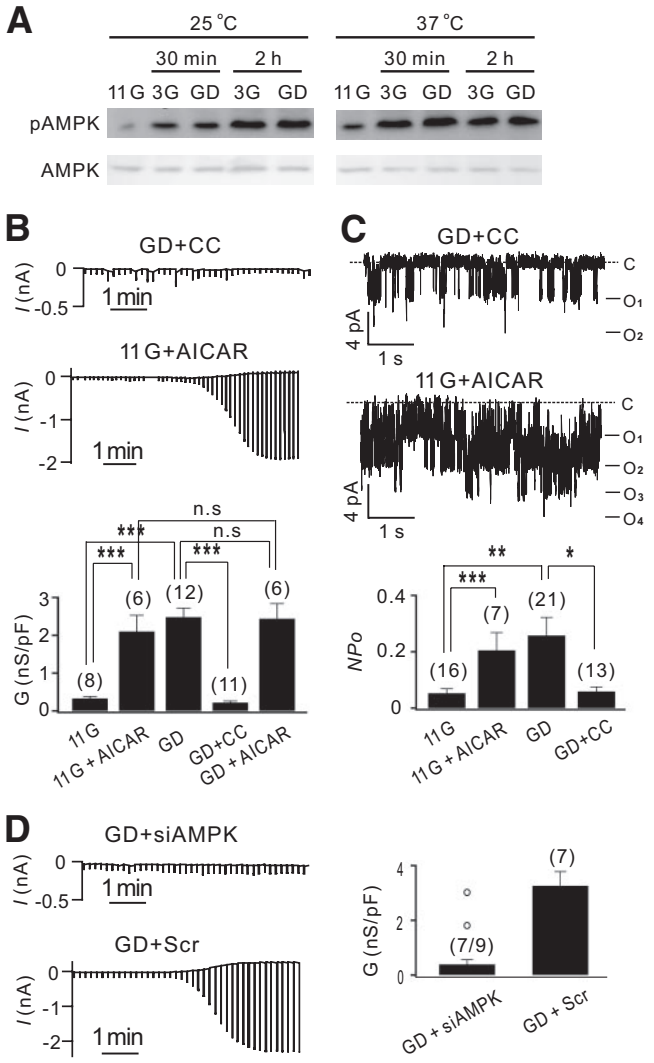

FIG. 2. Involvement of AMPK in GD-induced increases in K_{ATP} conductance. *A*: The levels of phosphorylated AMPK (*upper panel*) and total AMPK (*lower panel*) measured by Western blot assay from cell lysates of INS-1 cells pretreated with 3G or GD solution for the times indicated at room temperature (25°C, *left panel*) and 37°C (*right panel*). *B*: K_{ATP} whole-cell currents recorded in cells pretreated with compound C (10 μmol/l) in glucose-free solution (GD + CC, *upper panel*) and in cells pretreated with AICAR (0.5 mmol/l) in 11.1 mmol/l glucose solution (11G + AICAR, *middle panel*). Compound C and AICAR were present during the current recording. *Lower panel*: Normalized mean conductance (nS/pF) obtained in GD + CC (0.22 ± 0.04; $n = 11$), 11G + AICAR (2.10 ± 0.43; $n = 6$), and GD + AICAR (2.44 ± 0.40; $n = 6$) are compared with those of GD and 11G shown in Fig. 1*C*. *C*: Single K_{ATP} channel currents recorded at −60 mV in an inside-out patch obtained from GD + CC (*upper panel*) and 11G + AICAR treated INS-1 cells (*middle panel*). Mean values for *NPo* obtained in GD + CC (0.06 ± 0.02; $n = 13$) and 11G + AICAR (0.20 ± 0.06; $n = 7$) are compared with those of GD and 11G shown in Fig. 1*E*. *C*, closed level. *D*: Whole-cell current traces obtained from INS-1 cells transfected with Scr or siAMPK and pretreated in zero glucose for 2 h. Normalized G_{max} (in nS/pF); 0.39 ± 0.17 ($n = 7$) in siAMPK-transfected GD cells and 3.26 ± 0.52 ($n = 7$) in Scr-transfected GD cells. The G_{max} values in two GD + siAMPK cells that display exceptionally large currents are indicated separately by open circles above the bar. Statistical significance was evaluated by unpaired *t* test and one-way ANOVA. *$P < 0.05$, **$P < 0.01$, ***$P < 0.001$.

nine cells (Fig. 2*D*, *upper panel*). In two cells, K_{ATP} current activation was well observed, probably because of the variation in AMPK knockdown levels among cells. The G_{max} values in these cells were not included in the calculation of the mean value and are shown separately with open circles above the bar (Fig. 2*D*, *right panel*).

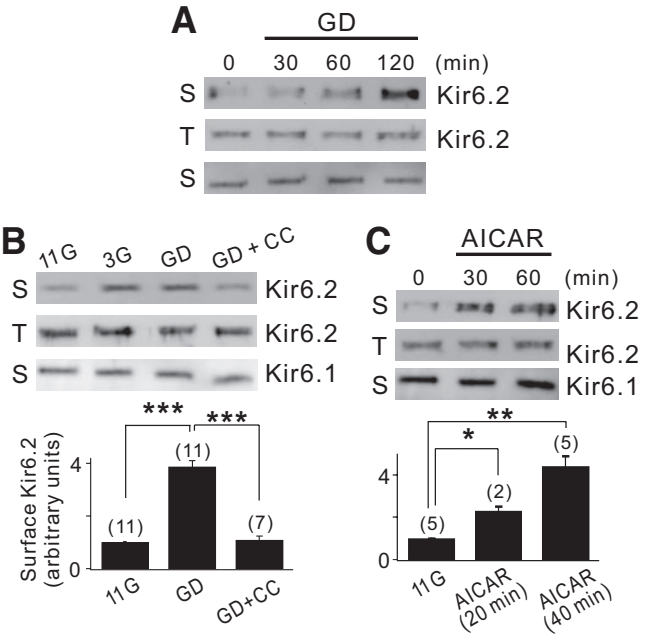

FIG. 3. Glucose deprivation increases the surface expression level of Kir6.2 through AMPK activation. *A*: INS-1 cells were incubated with GD medium for the times indicated before surface labeling with a biotin probe. The surface (S) or total (T) expression level of Kir6.2 was assessed by Western blot analysis as described in the online appendix. Kir2.1, a surface channel that does not react on glucose deprivation, was used as a negative control. *B*: The cells were maintained with 11G, 3G, or GD medium in the presence or absence of 40 μmol/l compound C for 2 h before surface labeling with a biotin probe. The surface expression level of Kir6.2 was quantified by densitometry and expressed as an arbitrary value to that of the cells incubated with GD medium, which was set to 1. Statistical significance was determined by ANOVA. ***$P < 0.001$. *C*: The cells were treated with 0.5 mmol/l AICAR-containing 11G medium for the times indicated before surface labeling with a biotin probe. The surface expression level of Kir6.2 was quantified by using the same method in *B*. Statistical significance was determined by ANOVA. *$P < 0.05$, **$P < 0.01$.

AMPK increases surface levels of K_{ATP} channel proteins. In principle, higher K_{ATP} channel activity can be caused by increasing the number of functional channels (*N*) or by increasing the open probability (*Po*). Because the measurement of G_{max} or *NPo* cannot distinguish these two possibilities (further discussion in the online appendix), we examined changes in the surface expression levels of Kir6.2 using surface biotinylation/streptavidin purification and subsequent Western blot analysis in INS-1 cells. For the loading control, we probed the same blots with an antibody to Kir2.1, another inward-rectifying K^+ channel. We found that the Kir6.2 surface levels were low in 11G- or 6G-treated cells (supplementary Fig. S5*B*) but increased similarly in 3G- and GD-treated cells (duration of pretreatment: 2 h; Fig. 3*B*). The increase in Kir6.2 surface level was dependent on the duration of glucose deprivation up to 2 h (Fig. 3*A*), which was consistent with the effect of glucose deprivation on AMPK activation (Fig. 2*A*). In contrast, the increase in surface Kir6.2 by glucose deprivation was abolished by compound C (duration of compound C application: 20 min in Fig. 3*B* and 5 min in supplementary Fig. S5*B*). Increased Kir6.2 surface expression was not induced by inducing hyperpolarization using a K_{ATP} channel opener (diazoxide; supplementary Fig. S5*B*) but induced by the addition of AICAR to 11G solution (Fig. 3*C*). Kir2.1 surface levels remained unchanged by these treatments, indicating that the above effects were specific to Kir6.2. We also verified that the total Kir6.2

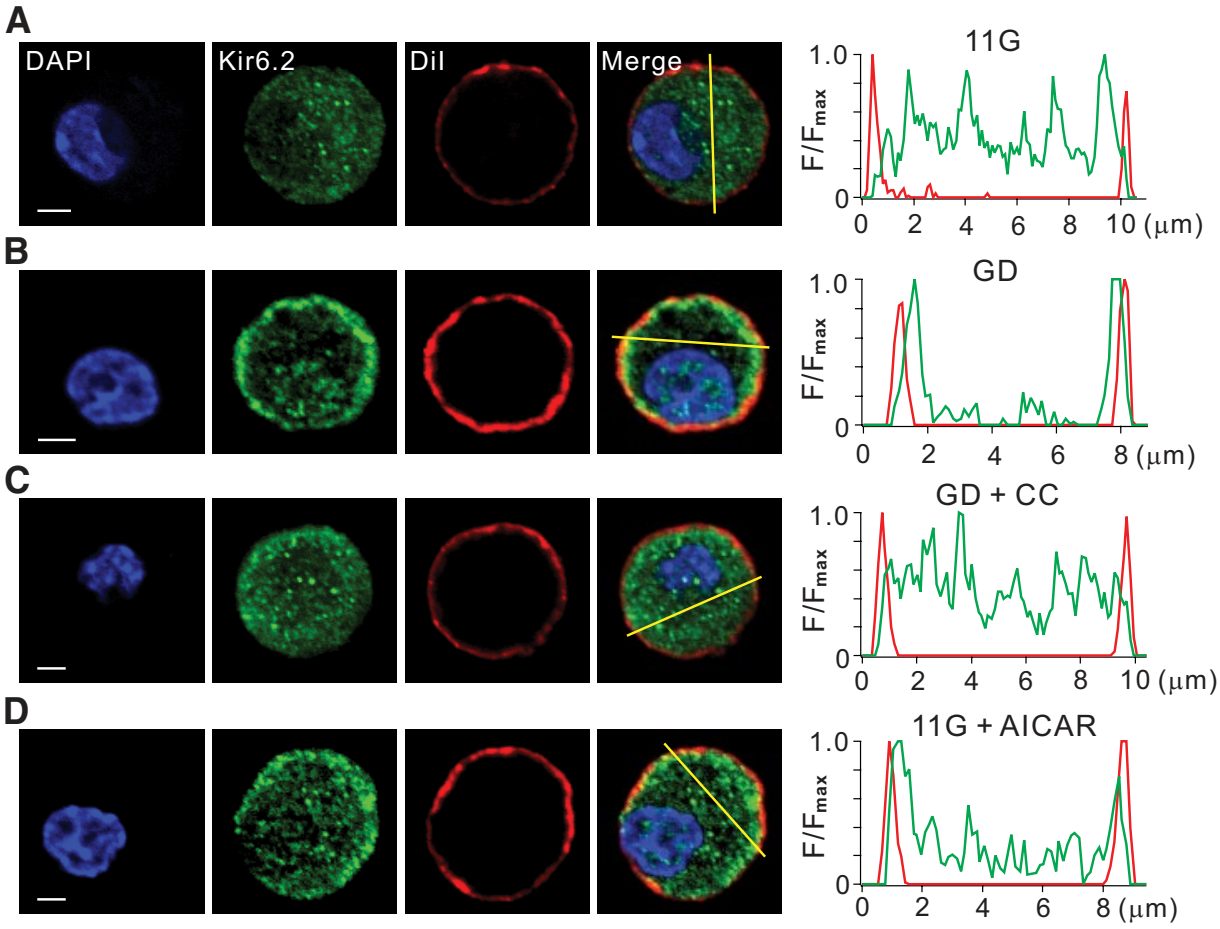

FIG. 4. AMPK increases surface localization of K_{ATP} channel proteins. *A–D*: Confocal fluorescent images obtained from pancreatic β-cells immunolabeled with Kir6.2 antibody (green, *second panel*) in 11G (*A*), GD (*B*), GD + CC (*C*), and 11G + AICAR (*D*). Both compound C (10 μmol/l) and AICAR (0.5 mmol/l) were pretreated for 1 h before fixation. Nucleus was stained with DAPI (blue, *first panel*), and plasma membrane was stained with DiI (red, *third panel*). Cells were incubated with these dyes (DAPI, 405-nm excitation, 1:5,000, molecular probes; DiI, 543-nm excitation, 1:1,000, Sigma) for 5 min immediately before mounting. Overlay of the fluorescence images showing Kir6.2, DAPI, and DiI (*fourth panel*). The intensity profiles of Kir6.2 (green) and DiI (red) fluorescence measured along a yellow line drawn across the cell membrane excluding the nucleus (*fifth panel*). Scale bar = 2 μm. (A high-quality color digital representation of this figure is available in the online issue.)

levels detected by directly immunoblotting the cell lysates did not change under these conditions, indicating that the AMPK-induced signaling activated during 3G or GD treatments regulated Kir6.2 trafficking to increase the Kir6.2 surface levels without changes in gene expression.

To observe changes in channel protein distributions, we used confocal microscopy with fluorescent-labeled antibodies to Kir6.2 (green) in pancreatic β-cells. The nucleus and plasma membrane were located using DiI (red) and DAPI (blue), respectively. In 11G-treated cells, punctuate structures were observed scattered in the cytosol (Fig. 4*A*), whereas in GD-treated cells, dominant fluorescence signals were observed at the cell periphery (Fig. 4*B*). The fluorescence intensity profiles measured along a line drawn across the cell membrane excluding the nucleus also confirmed that the areas of high intensity were scattered randomly in 11G-treated cells and at the cell periphery in GD-treated cells. The Kir6.2 signals at the cell periphery exhibited broader signal intensity than the red fluorescence signals emitted by plasma membrane marker DiI, suggesting that the amount Kir6.2 subunits underneath the membrane, as well as integrated at the surface membrane, were higher in GD-treated cells. Distribution of Kir2.1 subunits was not affected by glucose deprivation (supplementary Fig. S6). When compound C was added to the glucose-deprived medium, the effects of glucose deprivation on the distribution of Kir6.2 subunits were abolished (Fig. 4*C*). When AICAR was added to the 11G solution, the distribution pattern and intensity profile of Kir6.2 subunits were similar to those of GD-treated cells (Fig. 4*D*). Taken together, these results indicate that AMPK activation increases K_{ATP} channel surface expression by regulating the trafficking of K_{ATP} channel proteins. We confirmed that SUR1 distribution was changed by each treatment similarly to those observed for Kir6.2 subunits (supplementary Fig. S7).

Effects of compound C and AICAR on insulin secretion during glucose deprivation. To test the functional significance of the AMPK-dependent modulation of K_{ATP} channels, we examined whether compound C and AICAR cause decreases in insulin secretion in response to glucose deprivation (Fig. 5). The levels of released insulin were measured from rat pancreatic islets at 30-min intervals. The insulin secretion measured at 11.1 mmol/l glucose was higher in the presence of compound C, but lower in the presence of AICAR when compared with the control. After glucose deprivation, the release of insulin decreased gradually to the minimum level within 1 h for the control; this response was inhibited significantly by compound C,

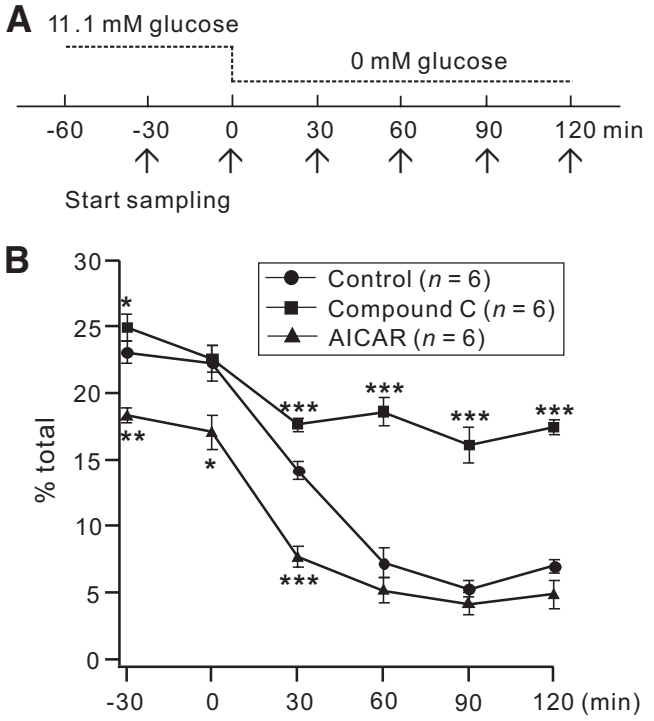

FIG. 5. Effects of compound C and AICAR on decreased insulin secretion because of glucose deprivation. *A*: Experimental protocol showing of how islets were incubated in 11.1 mmol/l glucose for 1 h before removing the glucose (time set as 0 min). The samples for insulin measurements were taken from each independent batch at −30, 0, 30, 60, 90, and 120 min (arrows) in the KRB buffer. *B*: Time-dependent changes in the percentage of islet insulin content secreted during acute glucose deprivation. Values represent the amount of secreted insulin during 30 min before each time point. Insulin secretion and final insulin content were quantified by an enzyme immunoassay. Insulin secretion as a percentage of total insulin content (secreted/total) was calculated. Control (circles); in the presence of compound C (triangles); in the presence of AICAR (squares). For each data point $n = 6$. *$P < 0.05$, **$P < 0.01$, ***$P < 0.001$ compared with the control.

whereas pretreatment with AICAR facilitated the decrease in insulin secretion in response to glucose deprivation.

DISCUSSION

Activity-dependent and cell signal-dependent trafficking has been reported for many cell surface channels (e.g., TRPC5) (22), transporters (e.g., GLUT4) (23), and receptors (e.g., AMPA receptors) (24), and these mechanisms play important roles in regulating their activities. The regulatory mechanisms for K_{ATP} channels have been investigated intensely for many years. Most studies have focused on direct regulation, such as changes in the open probability or the ATP sensitivity of the channels (25,26), but little is known about how channel numbers at the surface membrane are regulated. To investigate this aspect, we applied current recording, immunocytochemistry, and surface biotinylation techniques. Our results demonstrate that in pancreatic β-cells, the surface level of K_{ATP} channels is dynamically regulated by energy deprivation, resulting in higher K_{ATP} conductance. AMPK is involved in this regulation. Thus, we propose that the activation of K_{ATP} channels by energy depletion occurs in two steps: AMPK-dependent trafficking followed by channel opening via a decrease in ATP (supplementary Fig. S8).

The effects of glucose concentration on K_{ATP} channels in pancreatic β-cells have been investigated previously (8,27), but the results between studies are not entirely consistent. Smith et al. (27) reported that an acute reduction of glucose levels induced a rapid increase in the expression of both Kir6.2 and SUR1, and this effect was mimicked by the pharmacological activation of AMPK. These findings are consistent with ours, but they interpreted the results to indicate that glucose deprivation upregulates the translation of existing mRNAs because they observed no changes in channel distributions or mRNAs levels. In contrast, Yang et al. (8) reported that the incubation of β-cells in high-glucose solution (17 mmol/l) for 1 h resulted in increased Kir6.2 recruitment to the plasma membrane and increased K_{ATP} currents, and they claimed that PKA and Ca^{2+}-dependent signaling is involved in high-glucose–induced Kir6.2 recruitment. We do not know the exact reason for this discrepancy, but several important differences exist between experimental conditions (summarized in supplementary Table S1). Differences in the cell model (mouse vs. rat; RINm5F vs. INS-1; different passage), pretreatment protocols (incubation time and temperature), and internal solution composition may account for such discrepancy (see further details in the online appendix). The seemingly contradictory results may imply that the regulation of the surface density of K_{ATP} channels involves a complex signaling network and should be considered as a major factor in the regulation of K_{ATP} channel activities.

Although the present study primarily addresses the trafficking regulation of K_{ATP} channels by AMPK, it does not exclude the possibility that AMPK-dependent signaling contributes to the regulation of K_{ATP} gating. We showed that the effect of AMPK signaling on *NPo* measured from excised patches was similar to that on surface Kir6.2 levels (Figs. 2 and 3), implying that the changes in *NPo* are mainly attributable to the changes in channel density. However, AMPK inhibition reduced the whole-cell K_{ATP} conductance more profoundly (Fig. 2*B* and *D*). This difference may imply that AMPK signaling in intact cells contributes not only to K_{ATP} channel trafficking but also to facilitating K_{ATP} channel gating. The underlying mechanisms remain to be investigated, but several possibilities can be postulated: AMPK may phosphorylate K_{ATP} channels to increase channel gating or regulate intracellular factors that can facilitate K_{ATP} channel opening, such as MgADP (28–30), phosphoinositides (26), and long-chain acyl-CoAs (31).

What is the functional significance of the AMPK-dependent modulation of K_{ATP} channels? In fact, the inhibition of insulin secretion in a low energy state is a key mechanism in preventing hypoglycemia. K_{ATP} channel opening in low ATP is generally believed to mediate these responses, but the IC_{50} for ATP blocking measured in excised patches (~20 μmol/l) is too low to explain K_{ATP} channel opening at zero or low glucose, in which $[ATP]_i$ is at least 0.8 mmol/l (30). Because the AMP:ATP ratio varies more sensitively than the ADP:ATP ratio (32), we postulate that the AMPK-dependent modulation of K_{ATP} channels demonstrated in the present study ought to serve as a more sensitive and efficient means of regulating pancreatic β-cell excitability and insulin secretion under low-glucose conditions. To test this possibility, we monitored the changes in insulin secretion in response to glucose deprivation and tested the effects of pretreatment with compound C or AICAR (Fig. 5). The results indicated that the reduced insulin secretion by glucose deprivation is significantly attenuated by compound C and facilitated by

AICAR. Our results appeared to be consistent with the previous studies showing that forced activation of AMPK inhibited, whereas compound C increased, glucose-stimulated insulin secretions (33–35). In those studies, however, metabolic effects of AMPK were considered to be primarily responsible for regulating insulin secretion. It has not been studied whether the effects of AMPK on K_{ATP} channel trafficking are involved in this inhibition, but it was shown that AMPK decreased the number of docked vesicles containing insulin (36,37). This and the present study indicate that AMPK regulates the trafficking of insulin vesicles and Kir6.2 in opposing directions, so as to optimize the β-cell functions in a low energy state. A similar pattern of concerted action of AMPK was reported in epithelia for GLUT4 and CFTR trafficking (11).

In conclusion, K_{ATP} channel trafficking is regulated by cellular energy status via AMPK, and this process may play a key role in inhibiting insulin secretion under low energy status. Although the underlying molecular mechanisms involved in AMPK-dependent K_{ATP} channel trafficking remain to be elucidated, this study provides new insights into the regulation of K_{ATP} channels in pancreatic β-cells.

ACKNOWLEDGMENTS

This work was supported by the National Research Laboratory Program (R0A-2004-000-10295-0) funded by the Korean Ministry of Education, Science and Technology. A.L. and S.-H.P. were supported by the BK21 Program from the Korean Ministry of Education and Human Resources Development.

No potential conflicts of interest relevant to this article were reported.

REFERENCES

1. Ashcroft FM, Rorsman P. Electrophysiology of the pancreatic β-cell. Prog Biophys Mol Biol 1989;54:87–143
2. Tucker SJ, Gribble FM, Zhao C, Trapp S, Ashcroft FM. Truncation of Kir6.2 produces ATP-sensitive K^+ channels in the absence of the sulphonylurea receptor. Nature 1997;387:179–183
3. Gribble FM, Tucker SJ, Ashcroft FM. The essential role of the Walker A motifs of SUR1 in K-ATP channel activation by Mg-ADP and diazoxide. Embo J 1997;16:1145–1152
4. Nichols CG, Shyng SL, Nestorowicz A, Glaser B, Clement JPt, Gonzalez G, Aguilar-Bryan L, Permutt MA, Bryan J. Adenosine diphosphate as an intracellular regulator of insulin secretion. Science 1996;272:1785–1787
5. Cartier EA, Conti LR, Vandenberg CA, Shyng SL. Defective trafficking and function of KATP channels caused by a sulfonylurea receptor 1 mutation associated with persistent hyperinsulinemic hypoglycemia of infancy. Proc Natl Acad Sci U S A 2001;98:2882–2887
6. Partridge CJ, Beech DJ, Sivaprasadarao A. Identification and pharmacological correction of a membrane trafficking defect associated with a mutation in the sulfonylurea receptor causing familial hyperinsulinism. J Biol Chem 2001;276:35947–35952
7. Mankouri J, Taneja TK, Smith AJ, Ponnambalam S, Sivaprasadarao A. Kir6.2 mutations causing neonatal diabetes prevent endocytosis of ATP-sensitive potassium channels. Embo J 2006;25:4142–4151
8. Yang SN, Wenna ND, Yu J, Yang G, Qiu H, Yu L, Juntti-Berggren L, Kohler M, Berggren PO. Glucose recruits K(ATP) channels via non-insulin-containing dense-core granules. Cell Metab 2007;6:217–228
9. Hu K, Huang CS, Jan YN, Jan LY. ATP-sensitive potassium channel traffic regulation by adenosine and protein kinase C. Neuron 2003;38:417–432
10. Hardie DG, Scott JW, Pan DA, Hudson ER. Management of cellular energy by the AMP-activated protein kinase system. FEBS Lett 2003;546:113–120
11. Hallows KR. Emerging role of AMP-activated protein kinase in coupling membrane transport to cellular metabolism. Curr Opin Nephrol Hypertens 2005;14:464–471
12. Luiken JJ, Coort SL, Koonen DP, van der Horst DJ, Bonen A, Zorzano A, Glatz JF. Regulation of cardiac long-chain fatty acid and glucose uptake by translocation of substrate transporters. Pflugers Arch 2004;448:1–15
13. Hallows KR, Raghuram V, Kemp BE, Witters LA, Foskett JK. Inhibition of cystic fibrosis transmembrane conductance regulator by novel interaction with the metabolic sensor AMP-activated protein kinase. J Clin Invest 2000;105:1711–1721
14. Carattino MD, Edinger RS, Grieser HJ, Wise R, Neumann D, Schlattner U, Johnson JP, Kleyman TR, Hallows KR. Epithelial sodium channel inhibition by AMP-activated protein kinase in oocytes and polarized renal epithelial cells. J Biol Chem 2005;280:17608–17616
15. Walker J, Jijon HB, Churchill T, Kulka M, Madsen KL. Activation of AMP-activated protein kinase reduces cAMP-mediated epithelial chloride secretion. Am J Physiol Gastrointest Liver Physiol 2003;285:G850–G860
16. Kurth-Kraczek EJ, Hirshman MF, Goodyear LJ, Winder WW. 5′ AMP-activated protein kinase activation causes GLUT4 translocation in skeletal muscle. Diabetes 1999;48:1667–1671
17. Russell RR, 3rd, Bergeron R, Shulman GI, Young LH. Translocation of myocardial GLUT-4 and increased glucose uptake through activation of AMPK by AICAR. Am J Physiol Heart Circ Physiol 1999;277:H643–H649
18. Salt IP, Johnson G, Ashcroft SJ, Hardie DG. AMP-activated protein kinase is activated by low glucose in cell lines derived from pancreatic β-cells, and may regulate insulin release. Biochem J 1998;335:533–539
19. Kozlowski RZ, Ashford ML. ATP-sensitive K(+)-channel run-down is Mg2+ dependent. Proc R Soc Lond B Biol Sci 1990;240:397–410
20. Zhou G, Myers R, Li Y, Chen Y, Shen X, Fenyk-Melody J, Wu M, Ventre J, Doebber T, Fujii N, Musi N, Hirshman MF, Goodyear LJ, Moller DE. Role of AMP-activated protein kinase in mechanism of metformin action. J Clin Invest 2001;108:1167–1174
21. Corton JM, Gillespie JG, Hawley SA, Hardie DG. 5-aminoimidazole-4-carboxamide ribonucleoside. A specific method for activating AMP-activated protein kinase in intact cells? Eur J Biochem 1995;229:558–565
22. Bezzerides VJ, Ramsey IS, Kotecha S, Greka A, Clapham DE. Rapid vesicular translocation and insertion of TRP channels. Nat Cell Biol 2004;6:709–720
23. Dugani CB, Klip A. Glucose transporter 4: cycling, compartments and controversies. EMBO Rep 2005;6:1137–1142
24. Kennedy MJ, Ehlers MD. Organelles and trafficking machinery for postsynaptic plasticity. Annu Rev Neurosci 2006;29:325–362
25. Shyng SL, Barbieri A, Gumusboga A, Cukras C, Pike L, Davis JN, Stahl PD, Nichols CG. Modulation of nucleotide sensitivity of ATP-sensitive potassium channels by phosphatidylinositol-4-phosphate 5-kinase. Proc Natl Acad Sci U S A 2000;97:937–941
26. Shyng SL, Nichols CG. Membrane phospholipid control of nucleotide sensitivity of KATP channels. Science 1998;282:1138–1141
27. Smith AJ, Partridge CJ, Asipu A, Mair LA, Hunter M, Sivaprasadarao A. Increased ATP-sensitive K^+ channel expression during acute glucose deprivation. Biochem Biophys Res Commun 2006;348:1123–1131
28. Kakei M, Kelly RP, Ashcroft SJ, Ashcroft FM. The ATP-sensitivity of K^+ channels in rat pancreatic β-cells is modulated by ADP. FEBS Lett 1986;208:63–66
29. Larsson O, Ammala C, Bokvist K, Fredholm B, Rorsman P. Stimulation of the KATP channel by ADP and diazoxide requires nucleotide hydrolysis in mouse pancreatic β-cells. J Physiol 1993;463:349–365
30. Tarasov AI, Girard CAJ, Ashcroft FM. ATP sensitivity of the ATP-sensitive K^+ channel in intact and permeabilized pancreatic β-cells. Diabetes 2006;55:2446–2454
31. Gribble FM, Proks P, Corkey BE, Ashcroft FM. Mechanism of cloned ATP-sensitive potassium channel activation by oleoyl-CoA. J Biol Chem 1998;273:26383–26387
32. Towler MC, Hardie DG. AMP-activated protein kinase in metabolic control and insulin signaling. Circ Res 2007;100:328–341
33. da Silva Xavier G, Leclerc I, Varadi A, Tsuboi T, Moule SK, Rutter GA. Role for AMP-activated protein kinase in glucose-stimulated insulin secretion and preproinsulin gene expression. Biochem J 2003;371:761–774
34. Jewell JL, Luo W, Oh E, Wang Z, Thurmond DC. Filamentous actin regulates insulin exocytosis through direct interaction with Syntaxin 4. J Biol Chem 2008;283:10716–10726
35. Lamontagne J, Pepin E, Peyot ML, Joly E, Ruderman NB, Poitout V, Madiraju SR, Nolan CJ, Prentki M. Pioglitazone acutely reduces insulin secretion and causes metabolic deceleration of the pancreatic β-cell at submaximal glucose concentrations. Endocrinology 2009;150:3465–3474
36. Thurmond DC, Gonelle-Gispert C, Furukawa M, Halban PA, Pessin JE. Glucose-stimulated insulin secretion is coupled to the interaction of actin with the t-SNARE (target membrane soluble *N*-ethylmaleimide-sensitive factor attachment protein receptor protein) complex. Mol Endocrinol 2003;17:732–742
37. Tsuboi T, da Silva Xavier G, Leclerc I, Rutter GA. 5′-AMP-activated protein kinase controls insulin-containing secretory vesicle dynamics. J Biol Chem 2003;278:52042–52051